Instanton effects on the heavy-quark static potential *

U. T. Yakhshiev[1,2;1)] Hyun-Chul Kim[1,2,3;2)] B. Turimov[1;3)] M. M. Musakhanov[4;4)] Emiko Hiyama[2;5)]

[1] Department of Physics, Inha University, Incheon 22212, Republic of Korea
[2] RIKEN Nishina Center, RIKEN, 2-1 Hirosawa, 351-0115 Saitama, Japan
[3] School of Physics, Korea Institute for Advanced Study (KIAS), Seoul 02455, Republic of Korea
[4] Theoretical Physics Department, National University of Uzbekistan, Tashkent-174, Uzbekistan

Abstract: We investigate instanton effects on the heavy-quark potential, including its spin-dependent part, based on the instanton liquid model. Starting with the central potential derived from the instanton vacuum, we obtain the spin-dependent part of the heavy-quark potential. We discuss the results of the heavy-quark potential from the instanton vacuum. Finally, we solve the nonrelativistic two-body problem, associated with the heavy-quark potential from the instanton vacuum. The instanton effects on the quarkonia spectra are marginal but are required for quantitative description of the spectra.

Keywords: instanton-induced interactions, heavy-quark potential, quarkonia

PACS: 12.38.Lg, 12.39.Pn, 14.40.Pq **DOI:** 10.1088/1674-1137/41/8/083102

1 Introduction

Heavy-quark physics has evolved into a new phase. Charmonium-like states, which are known as XYZ states [1–13] and quite possibly include exotic states, conventional bottomonia including the lowest-lying state η_b [14–20], and heavy pentaquark states [21] have been newly reported by various experimental collaborations (see also recent reviews [22–25]). These novel findings of heavy hadrons have renewed interest in heavy-quark spectra and have subsequently triggered a great deal of experimental and theoretical work (see for example the reviews in Refs. [26–30]). Among these newly observed heavy hadrons, conventional bottomonium $\eta_b(1S)$ is placed in a crucial position. Even though it is the lowest-lying bottomonium, it has been observed only very recently [14–18] and the precise measurement of its mass provides a subtle test for any theory about heavy quarkonia, based on quantum chromodynamics (QCD) [31–33].

Various theoretical methods for the quarkonium spectra have been developed over recent decades (see recent reviews [27–29, 34]), among which the potential model has been widely used for describing the properties of quarkonia [35, 36]. The form of the potential at short distances is governed by the Coulomb-like interaction arising from perturbative QCD (pQCD). At the lowest order, one-gluon exchange between a heavy quark and a heavy anti-quark is responsible for this Coulomb-like attraction [37–40]. The running coupling constant for the Coulomb-like interaction has been considered with higher order corrections in pQCD [41–45]. However, when the distance between the quark and the anti-quark increases, certain nonperturbative contributions should be taken into account in the potential. Quark confinement [46] is shown to be the most essential nonperturbative part, obtained at least phenomenologically from the Wilson loop for the heavy-quark potential, which rises linearly at large distances [35, 36]. This linearly rising potential has been studied extensively in lattice QCD [47–54].

There is yet another nonperturbative effect on the heavy-quark potential from instantons [55], which are known to be one of the most important topological ob-

Received 17 January 2017, Revised 16 April 2017

∗ Supported by Basic Science Research Program through the National Research Foundation (NRF) of Korea funded by the Korean government (Ministry of Education, Science and Technology, MEST), Grant Numbers 2016R1D1A1B03935053 (UY) and 2015R1D1A1A01060707 (HChK) and The work was also partly Supported by RIKEN iTHES Project

1) E-mail: yakhshiev@inha.ac.kr
2) E-mail: hchkim@inha.ac.kr
3) E-mail: bturimov@yahoo.com
4) E-mail: yousuf@uzsci.net
5) E-mail: hiyama@riken.jp

jects in describing the QCD vacuum. These instanton effects on the heavy-quark potential were already studied many years ago [56–58], spin-dependent aspects of the heavy-quark potential being emphasized. The central part of the heavy-quark potential was first derived [59], based on the instanton liquid model for the QCD vacuum [60–62]. In Ref. [59], the Wilson loop was averaged in the instanton ensemble to get the heavy-quark potential, which rises almost linearly as the relative distance between the quark and the antiquark increases, then it starts to get saturated. The results of Ref. [59] have also been simulated in lattice QCD [63–65]. Though the instanton vacuum does not explain quark confinement, it will play a certain role in describing the characteristics of quarkonia. The features of the instanton vacuum will be recapitulated briefly in the present work in the context of the quarkonium hyperfine mass splittings.

In this work, we will examine the instanton effects on the heavy-quark potential from the instanton vacuum, including the spin-dependent parts in addition to the central one. In fact, Eichten and Feinberg [58] derived an analytic form of the instanton contributions to the spin-dependent potential but were not able to compute them due to the difficulties of deriving the static energy or the central static potential induced from instantons. Diakonov et al. [59] calculated this central part of the heavy-quark potential from the instanton vacuum, as mentioned previously. Thus, in the present work, we want to obtain the instanton-induced spin-dependent parts of the heavy-quark potential, following closely Refs. [58, 59]. To derive the spin-dependent potential from the instanton vacuum, we first expand the matter part of the QCD Lagrangian for the heavy quark with respect to the inverse of a heavy-quark mass $(1/m_{\rm Q})$, as is usually done in heavy-quark effective theory (HQET). As was obtained from Ref. [59], the central part comes from the leading order in the heavy-quark expansion. The heavy-quark propagator or the Wilson loop being averaged over the instanton medium, the central part can be derived. The spin-dependent contributions arise from the order of $1/m_{\rm Q}^2$. As we will show in this work, the heavy-quark propagator is given as an integral equation. Expanding it in powers of $1/m_{\rm Q}^2$, we are able to compute the spin-dependent part of the heavy-quark potential as was first shown in Ref. [58]. We will evaluate these spin-dependent potentials and examine their behaviour. Then we will proceed to compute the instanton effects on the hyperfine mass splittings of quarkonia. Assuming that the interaction range between a heavy quark and a heavy anti-quark is smaller than the inter-instanton distance, we can easily deal with the effects of the instantons on the hyperfine mass splittings of the quarkonia. We find at least qualitatively that the instantons have definite effects on those of the charmonia, while those of the bottomonia acquire tiny effects from the instanton vacuum because of the heavier mass of the bottom quark.

The paper is organized in the following way. In Section 2, we explain how to derive the instanton effects on the heavy-quark potential systematically. We first review the results of Ref. [59] within the heavy-quark expansion. Then we show the corrections to the spin-dependent heavy-quark potential, which come from the $1/m_{\rm Q}^2$ order. In Section 3 we discuss the results of the instanton effects on the heavy-quark potential in detail and present the numerical method used to solve the Schrödinger equation. We also present the spectrum of low-lying charmonium states and the estimates of the hyperfine mass splittings of these states. Finally, in Section 4 we summarise the results and give a future outlook related to the present work.

2 Formalism

2.1 Heavy-quark propagator

We start with the matter part of the QCD Lagrangian for the heavy quark, given as

$$\mathcal{L}_{\Psi}=\bar{\Psi}(x)\left(\mathrm{i}\not{D}-m_{\rm Q}\right)\Psi(x), \tag{1}$$

where $\mathrm{i}\not{D}=\mathrm{i}\not{\partial}+\not{A}$ denotes the covariant derivative, $m_{\rm Q}$ stands for the mass of the heavy quark, and $\Psi(x)$ represents the field corresponding to the heavy quark. As was done in HQET [66, 67], we assume that the heavy-quark mass $m_{\rm Q}$ goes to infinity with the velocity v of the heavy quark fixed ($v^2=1$). Then we can decompose the heavy-quark field into the large component $h_v(x)$ and the small one $H_v(x)$ as follows

$$\Psi(x)=\mathrm{e}^{-\mathrm{i}m_{\rm Q}v\cdot x}\left[h_v(x)+H_v(x)\right], \tag{2}$$

which is just the Foldy-Wouthuysen transformation [68, 69] used in the nonrelativistic expansion in QED. The $h_v(x)$ and $H_v(x)$ fields are defined respectively as

$$h_v(x)=\mathrm{e}^{im_{\rm Q}v\cdot x}\left(\frac{1+\not{v}}{2}\right)\Psi(x), \tag{3}$$

$$\not{v}h_v(x)=h_v(x),$$

$$H_v(x)=\mathrm{e}^{\mathrm{i}m_{\rm Q}v\cdot x}\left(\frac{1-\not{v}}{2}\right)\Psi(x), \tag{4}$$

$$\not{v}H_v(x)=-H_v(x).$$

The velocity vector allows one also to split the covariant derivative into the longitudinal and transverse components as

$$\not{D}=\not{v}(v\cdot D)+\not{D}_{\perp}, \tag{5}$$

where $\not{D}_\perp=\gamma^\mu(g_{\mu\nu}-v_\mu v_\nu)D^\nu$. The transverse component of the covariant derivative satisfies the relations

$$(\mathrm{i}\not{D}_\perp)^2=-\boldsymbol{D}^2+\frac{1}{2}\sigma\cdot G=\boldsymbol{P}^2+\boldsymbol{\sigma}\cdot\boldsymbol{B},\ \mathrm{i}\not{D}_\perp(\mathrm{i}v\cdot D)\mathrm{i}\not{D}_\perp =\boldsymbol{E}\cdot\boldsymbol{D}+\boldsymbol{\sigma}\cdot(\boldsymbol{E}\times\boldsymbol{D}), \tag{6}$$

where $G_{\mu\nu}$ stands for the gluon field strength tensor. $\boldsymbol{E}$ and $\boldsymbol{B}$ denote the chromoelectric and chromomagnetic fields, respectively. Using the equations of motion, we can remove the small field $H_v(x)$ by the relation

$$H_v=\frac{1}{2m_{\mathrm{Q}}+\mathrm{i}v\cdot D}\mathrm{i}\not{D}_\perp h_v \tag{7}$$

or equivalently we can integrate out the H_v fields [67]. Thus, we arrive at the effective action expressed only in terms of the h_v fields

$$\mathcal{S}_{\mathrm{eff}}[h_v,A]=\int \mathrm{d}^4x\bar{h}_v\left[\mathrm{i}v\cdot D-\mathrm{i}\not{D}_\perp\frac{1}{2m_{\mathrm{Q}}+\mathrm{i}v\cdot D}\mathrm{i}\not{D}_\perp\right]h_v, \tag{8}$$

where the first term will provide the central contribution to the heavy-quark potential while the second term is responsible for the spin-dependent part.

Using the effective Lagrangian given in Eq. (8), we can define the heavy quark propagator as

$$\left[\mathrm{i}v\cdot D-\mathrm{i}\not{D}_\perp\frac{1}{2m_{\mathrm{Q}}+\mathrm{i}v\cdot D}\mathrm{i}\not{D}_\perp\right]S(x,y;A)=\delta^{(4)}(x-y). \tag{9}$$

If we assume that the heavy-quark mass is infinitely heavy, then the heavy-quark propagator in the leading order satisfies the following equation

$$(\mathrm{i}v\cdot D)S_0(x,y;A)=\delta^{(4)}(x-y) \tag{10}$$

and its solution in the rest frame $v=(1,\boldsymbol{0})$ is found to be

$$S_0(x,y;A_4)=P\exp\left(\mathrm{i}\int_{x_4}^{y_4}\mathrm{d}z_4A_4\right)\delta^{(3)}(\boldsymbol{x}-\boldsymbol{y}), \tag{11}$$

where A_4 is the time component of the gluon field in four-dimensional Euclidean space. Note that since we consider the instanton field, which is the classical solution in Euclidean space, we work in Euclidean space from now on. Equation (11) implies that the heavy quark propagates along the time direction. The full propagator $S(x,y;A)$ is then expressed as an integral equation as follows

$$S(x,y;A)=S_0(x,y,A)-\int \mathrm{d}^4zS_0(x,z;A)\times\left[\mathrm{i}\not{D}_\perp\frac{1}{2m_{\mathrm{Q}}+\mathrm{i}v\cdot D}\mathrm{i}i\not{D}_\perp\right]S(z,y;A). \tag{12}$$

Since m_{Q} is rather heavy, we can expand the full propagator (12) iteratively in powers of $1/m_{\mathrm{Q}}$, when we derive the spin-dependent heavy-quark potential.

2.2 Heavy-quark potential from the instanton vacuum

The static heavy-quark potential is defined as the expectation value of the Wilson loop in a manifestly gauge-invariant manner

$$V(r)=-\lim_{T\to\infty}\frac{1}{T}\ln\langle 0|\mathrm{Tr}\{W_C[A]\}|0\rangle, \tag{13}$$

where $W_C[A]$ denotes the Wilson loop expressed as

$$W_C[A]=P\exp\left(\mathrm{i}\oint_C\mathrm{d}z_\mu A_\mu(z)\right). \tag{14}$$

The path is usually taken to be a large rectangle $(T\times r)$ as drawn in Fig. 1 with $r=|\boldsymbol{x}_1-\boldsymbol{x}_2|=|\boldsymbol{y}_1-\boldsymbol{y}_2|$.

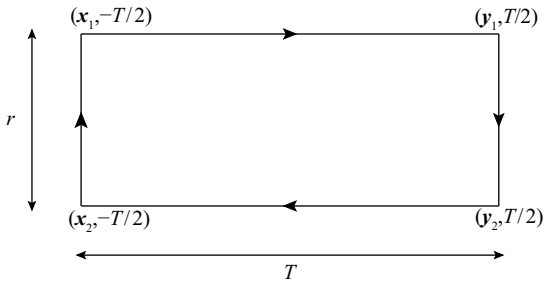

Fig. 1. The rectangular Wilson loop.

We first consider the central potential from the instanton vacuum, restating briefly the results from Ref. [59]. The leading-order expectation value of the Wilson loop in Euclidean space is defined as

$$\langle W_C[A]\rangle=\int DA_\mu\mathrm{Tr}P\exp\left(\mathrm{i}\oint_C\mathrm{d}x_\mu A_\mu(x)\right)\mathrm{e}^{-\mathcal{S}_{\mathrm{YM}}}, \tag{15}$$

where S_{YM} is the Yang-Mills action for the gluon field. The Wilson loop in the instanton medium can be written as

$$W_C[I,\bar{I}]=P\exp\left(\mathrm{i}\oint_C\mathrm{d}t\sum_{I,\bar{I}}a_{I,\bar{I}}\right), \tag{16}$$

where $a_{I,\bar{I}}=\dot{x}_\mu A_\mu^{I,\bar{I}}(x)$. I ($\bar{I}$) denotes the instanton (anti-instanton). $A_\mu^{I,\bar{I}}$ represent the instanton (anti-instanton) solutions of which the explicit expressions can be found in Appendix. The sum $\sum_{I,\bar{I}}a_{I,\bar{I}}$ stands for the superposition of N_+ instantons and N_- anti-instantons for the classical gluon background field $\bar{A}_\mu$, which is written as

$$\dot{x}_\mu\bar{A}_\mu(x,\xi)=\sum_{I=1}^{N_+}a_I(x,\xi)+\sum_{\bar{I}=1}^{N_-}a_{\bar{I}}(x,\xi), \tag{17}$$

where ξ represents the set of collective coordinates for the instanton, consisting of its center $z_{I\mu}$, the size ρ_I, and $SU(N_{\mathrm{c}})$ orientation matrix with the number of colors N_{c}. The integration over the gluon fields given in Eq. (15) is

then replaced with the integrations over the set of collective coordinates of the instantons (anti-instantons) [59–61] such that Eq. (15) can be understood as an average over the instanton ensemble.

The leading-order heavy-quark propagator in the rest frame is written in terms of the superposition of the instantons

$$S_0^{(i)}(x,y;a_{I,\bar{I}})=\langle y|\left(\frac{\mathrm{d}}{\mathrm{d}t}-\sum_{I,\bar{I}}a_{I,\bar{I}}^{(i)}+\mathrm{i}\epsilon\right)^{-1}|x\rangle, \tag{18}$$

where $a_{I,\bar{I}}^{(i)}$ represents the gluon field projected onto the corresponding ith Wilson line. Since $T\to\infty$, we can neglect the short sides of the rectangular path. The separation between the two long Wilson lines is given as r, as shown in Fig. 1. Using Eqs.(11) and (18), we can write the Wilson loop along the rectangle shown in Fig. 1 as

$$\mathrm{Tr}W_C=\Big\langle\!\Big\langle \mathrm{Tr}\big[S_0^{(1)}(\boldsymbol{x}_1,-T/2,\boldsymbol{y}_1,T/2;a_{I,\bar{I}})\times S_0^{(2)}(\boldsymbol{x}_2,-T/2,\boldsymbol{y}_2,T/2;a_{I,\bar{I}})\rangle\big]\Big\rangle\!\Big\rangle, \tag{19}$$

The double angle bracket $\langle\!\langle\cdots\rangle\!\rangle$ emphasizes the average over the instanton ensemble. Each heavy-quark propagator in Eq. (19) is expanded in powers of the instanton and anti-instanton fields $a_{I,\bar{I}}^{(1,2)}$. Then the sum of the planar diagrams is carried out, which is the leading order in the $1/N_\mathrm{c}$ expansion [70]. Note that the instanton vacuum has two parameters characterizing the dilute instanton liquid [60, 71]: the average size of the instanton $\bar{\rho}\simeq 0.33\mathrm{fm}$ and the average separation between instantons $\bar{R}=(N/V)^{-1/4}\simeq 1\mathrm{fm}$, where the instanton density is given as $N/V\simeq(200\mathrm{MeV})^4$. It allows one to use N/VN_c as a small perturbation parameter. We refer to Ref. [59] for further details of the calculation.

Using Eq. (A2), we can obtain the explicit form of the central potential from the instanton vacuum as

$$\begin{aligned}V_C&=\frac{N}{2VN_\mathrm{c}}\int\mathrm{d}^3z_I\mathrm{Tr}_\mathrm{c}\left[1-P\exp\left(\mathrm{i}\int_{-T/2}^{T/2}\mathrm{d}x_4A_{I4}^{(1)}\right)P\exp\left(-\mathrm{i}\int_{-T/2}^{T/2}\mathrm{d}x_4A_{I4}^{(2)}\right)\right]_{z_{I4}=0}+(I\to\bar{I})\\&=\frac{2N}{VN_\mathrm{c}}\int\mathrm{d}^3z\left[1-\cos\left(\frac{\pi|\vec{z}|}{\sqrt{|\vec{z}|^2+\bar{\rho}^2}}\right)\cos\left(\frac{\pi|\vec{z}+\vec{r}|}{\sqrt{|\vec{z}+\vec{r}|^2+\bar{\rho}^2}}\right)-\frac{\vec{z}(\vec{z}+\vec{r})}{|\vec{z}||\vec{z}+\vec{r}|}\sin\left(\frac{\pi|\vec{z}|}{\sqrt{|\vec{z}|^2+\bar{\rho}^2}}\right)\sin\left(\frac{\pi|\vec{z}+\vec{r}|}{\sqrt{|\vec{z}+\vec{r}|^2+\bar{\rho}^2}}\right)\right],\end{aligned} \tag{20}$$

where z denotes the position of the instanton, which is one of the collective coordinates for the instantons. The trace Tr_c runs over the colour space and r is the distance between the quark and antiquark. Further introducing the dimensionless variables $y=z/\bar{\rho}$ and $x=r/\bar{\rho}$, one can rewrite the potential in terms of the dimensionless integral $I(x)$

$$V_C(r)=\frac{4\pi N\bar{\rho}^3}{VN_\mathrm{c}}I\left(\frac{r}{\bar{\rho}}\right), \tag{21}$$

$$\begin{aligned}I(x)\;=\;&\int_0^\infty y^2\mathrm{d}y\int_{-1}^1\mathrm{d}t\left[1-\cos\left(\pi\frac{y}{\sqrt{y^2+1}}\right)\cos\left(\pi\sqrt{\frac{y^2+x^2+2xyt}{y^2+x^2+2xyt+1}}\right)\right.\\&\left.-\frac{y+xt}{\sqrt{y^2+x^2+2xyt}}\sin\left(\pi\frac{y}{\sqrt{y^2+1}}\right)\sin\left(\pi\sqrt{\frac{y^2+x^2+2xyt}{y^2+x^2+2xyt+1}}\right)\right].\end{aligned} \tag{22}$$

As r goes to infinity, the potential is saturated to be a constant

$$\lim_{r\to\infty}V_C(r)=2\Delta M_\mathrm{Q}, \tag{23}$$

where ΔM_Q is the correction to the heavy-quark mass from the instanton vacuum [59]

$$\begin{aligned}\Delta M_\mathrm{Q}&=\frac{N}{2VN_\mathrm{c}}\int\mathrm{d}^3z\mathrm{Tr}_\mathrm{c}\left[1-P\exp\left(\mathrm{i}\int_{-\infty}^{\infty}\mathrm{d}x_4A_{I4}\right)\Big|_{z_4=0}\right]+(I\to\bar{I})\\&=\frac{8\pi N\bar{\rho}^3}{VN_\mathrm{c}}\int_0^\infty\mathrm{d}yy^2\left(1+\cos\frac{\pi y}{\sqrt{y^2+1}}\right)=-\frac{4\pi^4N\bar{\rho}^3}{3VN_\mathrm{c}}\left(J_0(\pi)+\frac{1}{\pi}J_1(\pi)\right)\end{aligned} \tag{24}$$

calculated using again Eq. (A2). The average size of the instanton is regarded as the renormalization scale of the instanton vacuum [61, 72]. Keeping in mind the fact that the current quark mass is scale-dependent and its value is usually given at $\mu=m_\mathrm{c}$, certain scaling effects arising from the renormalization group equation for the

quark mass should be taken into account in order to estimate the effects on the heavy-quark mass from the instanton vacuum. The instanton effects should be slightly decreased when one matches the scale of $\Delta M_{\rm Q}$ to the charmed quark mass given in Ref. [73].

We are now in a position to consider the spin-dependent parts of the heavy-quark potential. The general procedure is very similar to what was done in Eq. (19). Since we consider now the finite heavy-quark mass, we need to use the full propagator given in Eq. (12) instead of the leading one. That is, we calculate the two Wilson lines as

$$\begin{aligned}{\rm Tr}W_C=&\Big\langle\!\Big\langle {\rm Tr}\big[S^{(1)}(\boldsymbol{x}_2,-T/2,\boldsymbol{y}_2,T/2;a_{I,\bar{I}})\\&\times S^{(2)}(\boldsymbol{x}_1,-T/2,\boldsymbol{y}_1,T/2;a_{I,\bar{I}})\rangle\big]\Big\rangle\!\Big\rangle. \end{aligned}\tag{25}$$

Considering the fact that $1/m_{\rm Q}$ can be regarded as a small parameter, we can expand the full propagators in Eq. (25) iteratively in powers of $1/m_{\rm Q}$. Using the relations given in Eq. (6), we first expand the term between S_0 and S in powers of $1/m_{\rm Q}$

$$\begin{aligned}{\rm i}\not{D}_\perp\frac{1}{2m_{\rm Q}+{\rm i}v\cdot D}{\rm i}\not{D}_\perp\approx&\frac{1}{2m_{\rm Q}}(-\boldsymbol{D}^2+\sigma\cdot\boldsymbol{B})\\&+\frac{1}{4m_{\rm Q}^2}[\boldsymbol{E}\cdot\boldsymbol{D}+\boldsymbol{\sigma}\cdot(\boldsymbol{E}\times\boldsymbol{D})].\end{aligned}\tag{26}$$

Then, the heavy-quark propagator for the ith Wilson loop can be iteratively expressed in powers of $1/m_{\rm Q}$ as

$$\begin{aligned}S^{(i)}(x,y;A)\approx&S_0^{(i)}(x,y;A)-\frac{1}{2m_{\rm Q}}\int{\rm d}^4\eta S_0^{(i)}(x,\eta;A)(-\boldsymbol{D}^2+\boldsymbol{\sigma}_i\cdot\boldsymbol{B})S_0^{(i)}(\eta,y;A)\\&-\frac{1}{4m_{\rm Q}^2}\int{\rm d}^4\eta S_0^{(i)}(x,\eta;A)(\boldsymbol{D}\cdot\boldsymbol{D}+\boldsymbol{\sigma}_i\cdot(\boldsymbol{E}\times\boldsymbol{D}))S_0^{(i)}(\eta,y;A)\\&+\frac{1}{4m_{\rm Q}^2}\int{\rm d}^4\eta{\rm d}^4\eta'\theta(\eta_4'-\eta_4)S_0^{(i)}(x,\eta;A)(-\boldsymbol{D}^2+\boldsymbol{\sigma}_i\cdot\boldsymbol{B})S_0^{(i)}(\eta,\eta';A)(-\boldsymbol{D}^2+\boldsymbol{\sigma}_i\cdot\boldsymbol{B})S_0^{(i)}(\eta',y;A).\end{aligned}\tag{27}$$

Replacing the full propagator in Eq. (25) with Eq. (27), we obtain the following expression

$$\begin{aligned}{\rm Tr}W_C=&\Big\langle\!\Big\langle {\rm Tr}\Big[S_0^{(1)}(\boldsymbol{x}_1,-T/2,\boldsymbol{y}_1,T/2;a_{I,\bar{I}})S_0^{(2)}(\boldsymbol{x}_2,-T/2,\boldsymbol{y}_2,T/2;a_{I,\bar{I}})\rangle\Big]\Big\rangle\!\Big\rangle\\&-\frac{1}{4m_{\rm Q}^2}\int{\rm d}^4\eta{\rm d}^4\eta'\Big\langle\!\Big\langle {\rm Tr}\Big[S_0^{(1)}(\boldsymbol{x}_1,-T/2,\boldsymbol{\eta},\eta_4;a_{I,\bar{I}})(-\boldsymbol{D}^2+\boldsymbol{\sigma}_1\cdot\boldsymbol{B})S_0^{(1)}(\boldsymbol{\eta},\eta_4,\boldsymbol{y}_1,T/2;a_{I,\bar{I}})\\&\times S_0^{(2)}(\boldsymbol{x}_2,-T/2,\boldsymbol{\eta},\eta_4;a_{I,\bar{I}})(-\boldsymbol{D}^2+\boldsymbol{\sigma}_2\cdot\boldsymbol{B})S_0^{(2)}(\boldsymbol{\eta},\eta_4,\boldsymbol{y}_1,T/2;a_{I,\bar{I}})\Big]\Big\rangle\!\Big\rangle\\&-\frac{1}{4m_{\rm Q}^2}\Big\langle\!\Big\langle {\rm Tr}\Big[S_0^{(1)}(\boldsymbol{x}_1,-T/2,\boldsymbol{y}_1,T/2;a_{I,\bar{I}})\int{\rm d}^4\eta S_0^{(2)}(\boldsymbol{x}_2,-T/2,\boldsymbol{\eta},\eta_4;a_{I,\bar{I}})(\boldsymbol{E}\cdot\boldsymbol{D}+\boldsymbol{\sigma}_2\cdot(\boldsymbol{E}\times\boldsymbol{D}))\\&\times S_0^{(2)}(\boldsymbol{\eta},\eta_4,\boldsymbol{y}_2,T/2;a_{I,\bar{I}})\Big]\Big\rangle\!\Big\rangle\\&-\frac{1}{4m_{\rm Q}^2}\Big\langle\!\Big\langle {\rm Tr}\Big[\int{\rm d}^4\eta S_0^{(1)}(\boldsymbol{x}_1-T/2,\boldsymbol{\eta},\eta_4;a_{I,\bar{I}})(\boldsymbol{E}\cdot\boldsymbol{D}+\boldsymbol{\sigma}_1\cdot(\boldsymbol{E}\times\boldsymbol{D}))S_0^{(1)}(\boldsymbol{\eta},\eta_4,\boldsymbol{y}_1,T/2;a_{I,\bar{I}})\\&\times S_0^{(2)}(\boldsymbol{x}_2,-T/2,\boldsymbol{y}_2,T/2;a_{I,\bar{I}})\Big]\Big\rangle\!\Big\rangle\\&+\frac{1}{4m_{\rm Q}^2}\Big\langle\!\Big\langle {\rm Tr}\Big[S_0^{(1)}(\boldsymbol{x}_1-T/2,\boldsymbol{y}_1,T/2;a_{I,\bar{I}})\int{\rm d}^4\eta{\rm d}^4\eta' S_0^{(2)}(\boldsymbol{x}_2,-T/2,\boldsymbol{\eta},\eta_4;a_{I,\bar{I}})(-\boldsymbol{D}^2+\boldsymbol{\sigma}_2\cdot\boldsymbol{B})\\&\times S_0^{(2)}(\boldsymbol{\eta},\eta_4,\boldsymbol{\eta}',\eta_4';a_{I,\bar{I}})(-\boldsymbol{D}^2+\boldsymbol{\sigma}_2\cdot\boldsymbol{B})S_0^{(2)}(\boldsymbol{\eta}',\eta_4',\boldsymbol{y}_2,T/2;a_{I,\bar{I}})\Big]\Big\rangle\!\Big\rangle\\&+\frac{1}{4m_{\rm Q}^2}\Big\langle\!\Big\langle {\rm Tr}\Big[\int{\rm d}^4\eta{\rm d}^4\eta' S_0^{(1)}(\boldsymbol{x}_1,-T/2,\boldsymbol{\eta},\eta_4;a_{I,\bar{I}})(-\boldsymbol{D}^2+\boldsymbol{\sigma}_1\cdot\boldsymbol{B})S_0^{(1)}(\boldsymbol{\eta},\eta_4,\boldsymbol{\eta}',\eta_4';a_{I,\bar{I}})\\&\times(-\boldsymbol{D}^2+\boldsymbol{\sigma}_1\cdot\boldsymbol{B})S_0^{(1)}(\boldsymbol{\eta}',\eta_4',,\boldsymbol{y}_1,T/2;a_{I,\bar{I}})S_0^{(2)}(\boldsymbol{x}_2,-T/2,\boldsymbol{y}_2,T/2;a_{I,\bar{I}})\Big]\Big\rangle\!\Big\rangle.\end{aligned}\tag{28}$$

Note that here we consider only the spin-dependent parts. For example, we can exclude the spin-independent term $\boldsymbol{D}^2/2m_{\rm Q}$, which is just the kinetic energy, and that proportional to $\boldsymbol{\sigma}\cdot\boldsymbol{B}$, which disappears because of parity invariance [58]. We can further simplify Eq. (28), leaving all spin-independent parts out, which are just part of the relativistic corrections to the potential. Taking only the spin-dependent parts into account, we obtain

$$
\begin{aligned}
\mathrm{Tr}W_C^{1/m_{\mathrm{Q}}^2}=&-\frac{1}{4m_{\mathrm{Q}}^2}\int \mathrm{d}^4\eta\mathrm{d}^4\eta' \Big\langle\!\Big\langle \mathrm{Tr}\Big[S_0^{(1)}(\boldsymbol{x}_1,-T/2,\boldsymbol{\eta},\eta_4;a_{I,\bar{I}})(-\boldsymbol{D}^2)S_0^{(1)}(\boldsymbol{\eta},\eta_4,\boldsymbol{y}_1,T/2;a_{I,\bar{I}})\\
&\times S_0^{(2)}(\boldsymbol{x}_2,-T/2,\boldsymbol{\eta},\eta_4;a_{I,\bar{I}})(\boldsymbol{\sigma}_2\cdot\boldsymbol{B})S_0^{(2)}(\boldsymbol{\eta},\eta_4,\boldsymbol{y}_1,T/2;a_{I,\bar{I}})\Big]\\
&+\mathrm{Tr}\Big[S_0^{(1)}(\boldsymbol{x}_1,-T/2,\boldsymbol{\eta},\eta_4;a_{I,\bar{I}})(\boldsymbol{\sigma}_1\cdot\boldsymbol{B})S_0^{(1)}(\boldsymbol{\eta},\eta_4,\boldsymbol{y}_1,T/2;a_{I,\bar{I}})\\
&\times S_0^{(2)}(\boldsymbol{x}_2,-T/2,\boldsymbol{\eta},\eta_4;a_{I,\bar{I}})(-\boldsymbol{D}^2)S_0^{(2)}(\boldsymbol{\eta},\eta_4,\boldsymbol{y}_1,T/2;a_{I,\bar{I}})\Big]\Big\rangle\!\Big\rangle\\
&+\mathrm{Tr}\Big[S_0^{(1)}(\boldsymbol{x}_1,-T/2,\boldsymbol{\eta},\eta_4;a_{I,\bar{I}})(\boldsymbol{\sigma}_1\cdot\boldsymbol{B})S_0^{(1)}(\boldsymbol{\eta},\eta_4,\boldsymbol{y}_1,T/2;a_{I,\bar{I}})\\
&\times S_0^{(2)}(\boldsymbol{x}_2,-T/2,\boldsymbol{\eta},\eta_4;a_{I,\bar{I}})(\boldsymbol{\sigma}_2\cdot\boldsymbol{B})S_0^{(2)}(\boldsymbol{\eta},\eta_4,\boldsymbol{y}_1,T/2;a_{I,\bar{I}})\Big]\Big\rangle\!\Big\rangle\\
&-\frac{1}{4m_{\mathrm{Q}}^2}\Big\langle\!\Big\langle \mathrm{Tr}\Big[S_0^{(1)}(\boldsymbol{x}_1,-T/2,\boldsymbol{y}_1,T/2;a_{I,\bar{I}})\\
&\times\int \mathrm{d}^4\eta S_0^{(2)}(\boldsymbol{x}_2,-T/2,\boldsymbol{\eta},\eta_4;a_{I,\bar{I}})(\boldsymbol{\sigma}_2\cdot(\boldsymbol{E}\times\boldsymbol{D}))S_0^{(2)}(\boldsymbol{\eta},\eta_4,\boldsymbol{y}_2,T/2;a_{I,\bar{I}})\Big]\Big\rangle\!\Big\rangle\\
&-\frac{1}{4m_{\mathrm{Q}}^2}\Big\langle\!\Big\langle \mathrm{Tr}\Big[\int \mathrm{d}^4\eta S_0^{(1)}(\boldsymbol{x}_1-T/2,\boldsymbol{\eta},\eta_4;a_{I,\bar{I}})(\boldsymbol{\sigma}_1\cdot(\boldsymbol{E}\times\boldsymbol{D}))S_0^{(1)}(\boldsymbol{\eta},\eta_4,\boldsymbol{y}_1,T/2;a_{I,\bar{I}})\\
&\times S_0^{(2)}(\boldsymbol{x}_2,-T/2,\boldsymbol{y}_2,T/2;a_{I,\bar{I}})\Big]\Big\rangle\!\Big\rangle. \qquad (29)
\end{aligned}
$$

The final expression for W_C^{1/m_{Q}^2} contains $1/m_{\mathrm{Q}}^2$, so that we can expand the exponential of Eq. (13) in powers of $1/m_{\mathrm{Q}}^2$. Then, Eq. (29) will lead to the spin-dependent parts of the heavy-quark potential from the instanton vacuum. The derivation of the potential from Eq. (29) is lengthy but straightforward. In Ref. [58], it was shown in detail how one can obtain the spin-dependent parts of the heavy-quark potential in QCD. Since the form of Eq. (29) is very similar to the corresponding one in Ref. [58], we will closely follow the method of Ref. [58] and refer to it. The leading-order propagator given in Eq. (11) is identified as the path-order exponential along the time direction apart from the Dirac delta function. Using the identities for the path-ordered exponentials given in the Appendix, we can proceed to compute each term in Eq. (29). Note that the instanton satisfies the self-duality condition $G^a_{\mu\nu}=\pm\tilde{G}^a_{\mu\nu}$ ($\boldsymbol{B}=\pm\boldsymbol{E}$), which plays an essential role in deriving the spin-dependent potential from the instanton vacuum. It makes it possible to relate several independent potentials to the central potential given in Eq. (21). As a result, all the spin-dependent potentials are expressed in terms of the central potential

$$
\begin{aligned}
V_{SD}(\boldsymbol{r})=&\frac{1}{4m_{\mathrm{Q}}^2}(\boldsymbol{L}_1\cdot\boldsymbol{\sigma}_2-\boldsymbol{L}_2\cdot\boldsymbol{\sigma}_1)\frac{1}{r}\frac{\mathrm{d}V_C(r)}{\mathrm{d}r}+\frac{\boldsymbol{\sigma}_1\cdot\boldsymbol{\sigma}_2}{12m_{\mathrm{Q}}^2}\nabla^2V_C(r)\\
&+\frac{1}{3m_{\mathrm{Q}}^2}(3\boldsymbol{\sigma}_1\cdot\boldsymbol{n}\boldsymbol{\sigma}_2\cdot\boldsymbol{n}-\boldsymbol{\sigma}_1\cdot\boldsymbol{\sigma}_2)\left(\frac{1}{r}\frac{\mathrm{d}}{\mathrm{d}r}-\frac{\mathrm{d}^2}{\mathrm{d}r^2}\right)V_C(r), \qquad (30)
\end{aligned}
$$

where $\boldsymbol{L}_i$ and $\boldsymbol{\sigma}_i$ represent respectively the orbital angular momentum and the Pauli spin operator of the corresponding heavy quark, and $\boldsymbol{n}$ designates the unit radial vector. The potential $V_C(r)$ denotes the central part of the potential that we already have shown in Eq. (21). We have used $m_{\mathrm{Q}}=m_{\bar{\mathrm{Q}}}$. If one considers two heavy quarks with different masses, we can simply replace m_{Q}^2 with $m_{\mathrm{Q}}m_{\bar{\mathrm{Q}}}$ in Eq. (30).

The spin-dependent potential V_{SD} can be now decomposed into three different parts, i.e., the spin-spin interaction $V_{SS}(r)$, the spin-orbit coupling term $V_{LS}(r)$, and the tensor part $V_T(r)$:

$$
\begin{aligned}
V_{\mathrm{Q}\bar{\mathrm{Q}}}(\boldsymbol{r})=&V_C(r)+V_{SS}(r)(\boldsymbol{S}_{\mathrm{Q}}\cdot\boldsymbol{S}_{\bar{\mathrm{Q}}})+V_{LS}(r)(\boldsymbol{L}\cdot\boldsymbol{S})\\
&+V_T(r)[3(\boldsymbol{S}_{\mathrm{Q}}\cdot\boldsymbol{n})(\boldsymbol{S}_{\bar{\mathrm{Q}}}\cdot\boldsymbol{n})-\boldsymbol{S}_{\mathrm{Q}}\cdot\boldsymbol{S}_{\bar{\mathrm{Q}}}], \qquad (31)
\end{aligned}
$$

where $\boldsymbol{S}_{\mathrm{Q}(\bar{\mathrm{Q}})}$ stands for the spin of a heavy quark (heavy anti-quark) $\boldsymbol{S}_{\mathrm{Q}(\bar{\mathrm{Q}})}=\boldsymbol{\sigma}_{1(2)}/2$, $\boldsymbol{S}$ is their total spin $\boldsymbol{S}=\boldsymbol{S}_1+\boldsymbol{S}_2$, and $\boldsymbol{L}$ represents the relative orbital angular momentum $\boldsymbol{L}=\boldsymbol{L}_1-\boldsymbol{L}_2$. Each potential of Eq. (31) is defined respectively as

$$
\begin{aligned}
V_{SS}(r)=&\frac{1}{3m_{\mathrm{Q}}^2}\nabla^2V_C(r),\\
V_{LS}(r)=&\frac{1}{2m_{\mathrm{Q}}^2}\frac{1}{r}\frac{\mathrm{d}V_C(r)}{\mathrm{d}r},\\
V_T(r)=&\frac{1}{3m_{\mathrm{Q}}^2}\left(\frac{1}{r}\frac{\mathrm{d}V_C(r)}{\mathrm{d}r}-\frac{\mathrm{d}^2V_C(r)}{\mathrm{d}r^2}\right). \qquad (32)
\end{aligned}
$$

Thus, all three components of the spin-dependent potential are expressed in terms of the central potential $V_C(r)$.

3 Numerical calculations, results and discussions

3.1 Instanton potential

In the instanton liquid model for the QCD vacuum, we have two important parameters, i.e., the average size of the instanton $\bar{\rho}\simeq 0.33$fm and the average

distance $\bar{R}\simeq 1$fm between instantons, as we have already mentioned. These numbers were first proposed by Shuryak [71] within the instanton liquid model and were derived from $\Lambda_{\overline{MS}}$ by Diakonov and Petrov [60]. Thus, it is also of great interest to look into the dependence of the heavy-quark potential from the instanton vacuum on these parameters. Moreover, the values given above should not be considered as the exact ones. For example, Refs. [80–82] considered $1/N_{\rm c}$ meson-loop contributions in the light-quark sector and found it necessesary to readjust the values of the parameters as $\bar{\rho}\simeq 0.35$fm and $\bar{R}\simeq 0.856$fm. Lattice simulations of the instanton vacuum suggested $\bar{\rho}\approx 0.36$fm and $\bar{R}\approx 0.89$fm [83–86], which is almost the same as those with the $1/N_{\rm c}$ meson-loop corrections. Thus, we want to examine the dependence of the heavy-quark potential from the instanton vacuum on three different sets of parameters, that is, Set I [60, 71], Set IIa [80–82], and Set IIb [83–86]. The parameter dependence of the potential can be easily understood from the form of the leading-order potential expressed in Eq. (21). While the prefactor $\bar{\rho}^3/\bar{R}^4N_{\rm c}$, which includes both the parameters, governs the overall strength of the potential, its range is dictated only by the instanton size $\bar{\rho}$ through the dimensionless integral $I(r/\bar{\rho})$.

When the quark-antiquark distance is smaller than the instanton size, i.e., $r\ll\bar{\rho}$ ($x\ll 1$), one can expand the dimensionless integral $I(x)$ with respect to x

$$I(x)\simeq\left[\frac{\pi^3}{48}-\frac{\pi^3}{3}J_1(2\pi)\right]x^2 +\left[-\frac{\pi^3(438+7\pi^2)}{30720}+\frac{J_2(2\pi)}{80}\right]x^4+\mathcal{O}(x^6), \quad (33)$$

which yields the central potential in the form of a polynomial

$$V_C(r)\simeq\frac{4\pi\bar{\rho}^3}{\bar{R}^4N_{\rm c}}\left(1.345\frac{r^2}{\bar{\rho}^2}-0.501\frac{r^4}{\bar{\rho}^4}\right). \quad (34)$$

As the distance between the quark and the antiquark grows larger than the intstanton size, i.e. $r\gg\bar{\rho}$ ($x\gg 1$), we again get an analytic expression as follows

$$I(x)\simeq-\frac{2\pi^2}{3}\Big[\pi J_0(\pi)+J_1(\pi)\Big]-\frac{\pi^2}{2x}+\mathcal{O}(x^{-2}). \quad (35)$$

Consequently, the central potential at large r can be approximately written as

$$V(r)\simeq 2\Delta M_{\rm Q}-\frac{g_{\rm NP}}{r}. \quad (36)$$

The second term behaves like a Coulomb-like potential. So, crudely speaking, this can be understood as a nonperturbative contribution to the perturbative one gluon exchange potential from the instanton vauum at large r. The coupling constant $g_{\rm NP}$ in Eq.(36), which is defined as $g_{\rm NP}:=2\pi^3\bar{\rho}^4/(N_{\rm c}\bar{R}^4)$, could be regarded as a nonperturbative correction to the strong coupling constant $\alpha_s(r)$. When r goes to infinity, $r\to\infty$, the potential is saturated at the value of $2\Delta M_{\rm Q}$. As discussed already in Ref. [59], this implies that the instanton vacuum cannot explain quark confinement. In the case of parameter Set I, which is often considered in the light-quark sector, the value of $\Delta M_{\rm Q}$ is found to be $\Delta M_{\rm Q}\simeq 66.6$MeV. However, if one chooses Set IIa, then the result becomes $\Delta M_{\rm Q}\simeq 143.06$MeV. The Set IIb produces $\Delta M_{\rm Q}\simeq 135.72$MeV.

Figure 2 shows the r dependence of each term of the heavy-quark potentials from the instanton vacuum. We consider the charm quark sector as an example. We also show the dependence of each term of the potential on two different sets of parameters, that is, Set I and Set IIb. One can see that the central part of the potential increases monotonically at small distances $r\ll\bar{\rho}$ and later becomes almost linear at distances comparable with the instanton size $r\sim\bar{\rho}$, as already discussed in Ref. [59]. At large $r\gg\bar{\rho}$ it starts to get saturated at the value $V_C(r\to\infty)\simeq 133.2$MeV with Set I and $V_C(r\to\infty)\simeq 271.44$MeV with Set IIb. The spin-spin interaction part is of particular interest among these contributions to the spin-dependent potential. In pQCD, it is given as a point-like interaction [87] at leading order. The spin-spin interaction from the instanton vacuum, though, looks similar to a Gaussian-type interaction. The spin-orbit potential behaves in a similar way to the spin-spin potential. The tensor interaction, however, shows a different r dependence. As r increases, the tensor potential vanishes at $r=0$ and then starts to increase until $r\approx 0.4$fm, from which it begins to fall off. The strength of each part of the potential become stronger when a smaller value of $\bar{R}$ is employed, since all terms turn out to be very sensitive to $\bar{R}$ on account of the prefactor $\bar{\rho}^3/\bar{R}^4N_{\rm c}$. This implies that a less dilute instanton medium yields stronger interactions between a heavy quark and a heavy antiquark. However, one has to keep in mind that the value of $\bar{R}$ should not be continually decreased, because the whole framework of the instanton liquid model is based on the diluteness of the instanton medium, where the packing parameter proportional to $(\bar{\rho}/\bar{R})^4$ must be kept small.

The change of the $\bar{\rho}$ value seems less effective in the spin-dependent parts of the potential, however. This is again due to the fact that all spin-dependent parts have the prefactor $\bar{\rho}/\bar{R}^4N_{\rm c}$, where instanton size appears in the first order, after rewriting the spin-dependent parts in terms of the dimensionless integral $I(x)$ (see Eq. (22)) and its derivatives. As mentioned in the previous section, the average size of the instanton has a physical meaning as the renormalization scale [61, 72], which is a crucial virtue of the instanton liquid model. Thus, $\bar{\rho}=0.33$fm indicates a renormalization scale $\mu=600$ MeV. Bearing

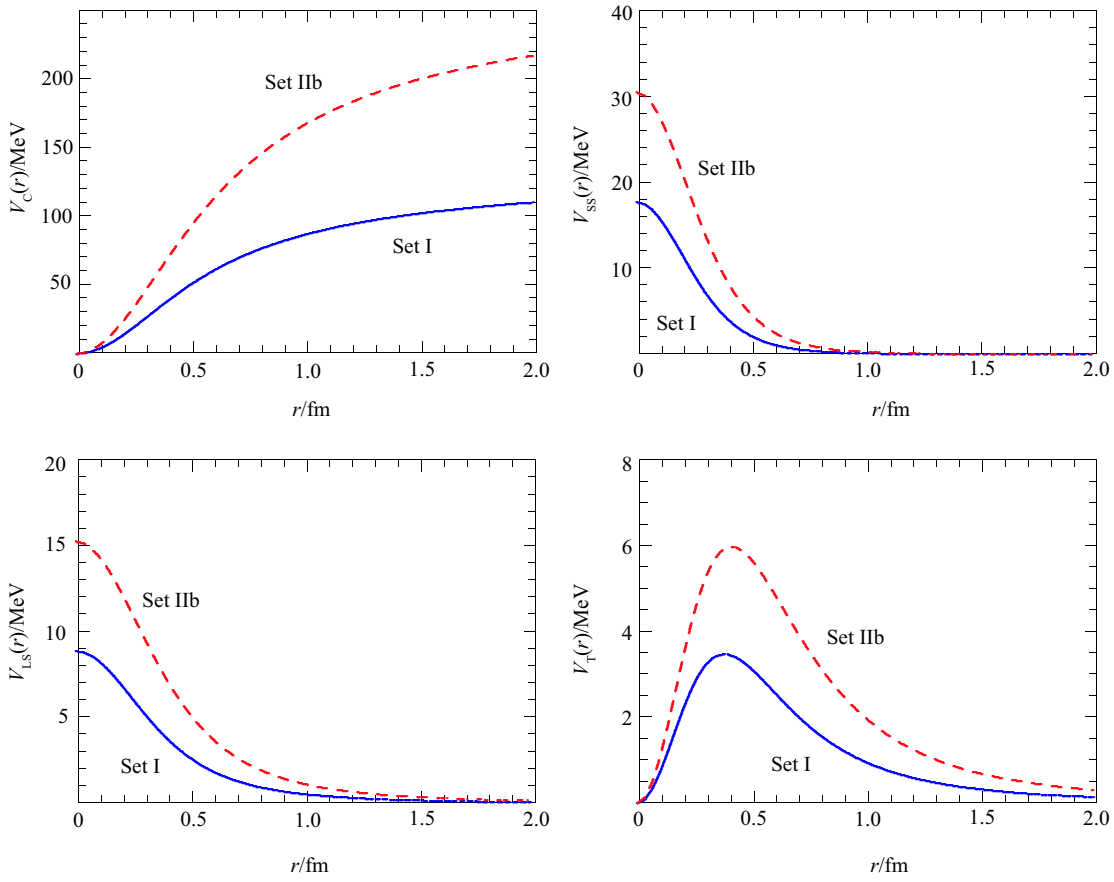

Fig. 2. Each contribution to the heavy-quark potential as a function of r for the two different sets of instanton parameters $\bar{\rho}$ and $\bar{R}$. The upper-left panel depicts the central part of the potential, the upper-right panel the spin-spin interaction, the lower-left panel the spin-orbit part, and the lower-right one the tensor interaction. The solid curve corresponds to Set I with ρ=0.33 fm and $\bar{R}$=1fm from the phenomenology [60, 71], whereas the dashed one corresponds to Set IIb with ρ=0.36 fm and $\bar{R}$=0.89fm from the lattice simulations [83–86]. The mass of the charm quark is chosen to be m_c=1275 MeV.

in mind this meaning of $\bar{\rho}$, we should not take the value of $\bar{\rho}$ freely. Note that the value of $\bar{\rho}^{-1}$=600MeV implies the strong coupling constant is frozen at $\bar{\rho}^{-1}$. Thus, Fig. 2 shows the dependence of the heavy-quark potential on both $\bar{\rho}$ and $\bar{R}$ within the range of constraints on their values. In the case of the bottom quarks and anti-quarks, the instanton effects are highly suppressed because of the large bottom quark mass.

For completeness, we provide the expression for the matrix elements of the $Q\bar{Q}$ potential in Eq. (31)

$$\begin{aligned}\langle {}^{2S+1}L_J|V_{Q\bar{Q}}(\boldsymbol{r})|{}^{2S+1}L_J\rangle=&V(r)+\left[\frac{1}{2}S(S+1)-\frac{3}{4}\right]V_{SS}(r)+\frac{1}{2}[J(J+1)-L(L+1)-S(S+1)]V_{LS}(r)\\&\times\left\{-\frac{3[J(J+1)-L(L+1)-S(S+1)][J(J+1)-L(L+1)-S(S+1)+1]}{2(2L-1)(2L+3)}\right.\\&\left.+\frac{2S(S+1)L(L+1)}{(2L-1)(2L+3)}\right\}V_T(r),\end{aligned}\tag{37}$$

where we have used the conventional spectroscopic notation ${}^{2S+1}L_J$ given in terms of the total spin S, the orbital angular momentum L, and the total angular momentum J satisfying the relation $\boldsymbol{J}=\boldsymbol{L}+\boldsymbol{S}$.

3.2 Gaussian expansion method

In order to evaluate the bound states in the spectrum of quarkonia, we need to solve the Schrödinger equation with the potential from the instanton vacuum given in

Eq. (31)

$$\left[-\frac{\hbar^2}{m_{\rm Q}}\nabla^2+V_{\rm Q\bar{Q}}(\boldsymbol{r})-E\right]\Psi_{JM}(\boldsymbol{r})=0, \tag{38}$$

where $m_{\rm Q}$ arises from the doubled reduced mass of the quarkonium system and Ψ_{JM} represents the wave function of the state with total angular momentum J and its third component M. We can solve Eq. (38) numerically, using the Gaussian expansion method (see review in Ref. [89]) in which the wave function is expanded in terms of a set of L^2-integrable basis functions $\{\Phi^{LS}_{JM,n};n=1-n_{\rm max}\}$

$$\Psi_{JM}(\boldsymbol{r})=\sum_{n=1}^{n_{\rm max}}C^{(J)}_{n,LS}\Phi^{LS}_{JM,n}(\boldsymbol{r}) \tag{39}$$

and the Rayleigh-Ritz variational principle is employed. Thus, one can formulate a generalized eigenvalue problem given as

$$\sum_{m=1}^{n_{\rm max}}\langle\Phi^{LS}_{JM,n}\left|-\frac{\hbar^2}{m_{\rm Q}}\nabla^2+V_{\rm Q\bar{Q}}(\boldsymbol{r})-E\right|\Phi^{LS}_{JM,m}\rangle C^{(J)}_{m,LS}=0. \tag{40}$$

The normalized radial part of the basis wave functions $\phi^L_n(r)$ is expressed in terms of the Gaussian basis functions

$$\phi^L_n(r)=\left(\frac{2^{2L+\frac{7}{2}}r_n^{-2L-3}}{\sqrt{\pi}(2L+1)!!}\right)^{1/2}r^L{\rm e}^{-(r/r_n)^2}, \tag{41}$$

where $r_n, n=1,2,\cdots,n_{\rm max}$ stand for variational parameters. In the case of a two-body problem, the total number of variational parameters can be reduced by choosing the geometric progression in the form of $r_n=r_1a^{n-1}$, which produces a good convergence of the results. Thus, we need only three variational parameters, i.e. r_1, a and $n_{\rm max}$.

3.3 Quarkonium states

We already mentioned that at large distance the instanton potential is saturated, so that there is no confinement in the present approach. The bound or quasibound charmonium states with masses below or around the threshold mass $M_{\rm Q\bar{Q}}\simeq 2(m_{\rm c}+\Delta M_{\rm Q})$, where $m_{\rm c}=1275$ is the charm quark mass [73], are listed in Table 1 with the two different sets of the instanton parameters. Other states above threshold will appear as resonances in the present approach.

One can see that the instanton effects are not small in reproducing the mass of quarkonia. For example, in the case of the potential with parameter Set I, the contribution to the mass of a charmonium is determined by $\Delta M_{\rm c\bar{c}}=M_{\rm c\bar{c}}-2m_{\rm c}$. For example, the contribution of the instanton effects to the $\eta_{\rm c}$ mass turns out to be 118.81 MeV, which is approximately about 30% of the experimental value 433.60 MeV. As discussed already, the potential from the instanton vacuum is sensitive to the instanton parameters. Therefore, a change in the instanton parameters strongly affects the spectrum of $\rm Q\bar{Q}$ states. For example, parameter Set IIb gives the result $\Delta M_{\eta_{\rm c}}\simeq 203.64$ MeV, which is almost 50% of the experimental value. Parameter Set IIa gives slightly larger results than Set IIb. When it comes to the J/ψ state, the instanton effects on the $\rm Q\bar{Q}$ mass becomes smaller in comparison with the experimental data. However, it is still important to consider them, since $\Delta M_{\rm J/\psi}$ is 119.57 MeV (205.36 MeV) with Set I (Set IIb) used, compared with the experimental value 540.92 MeV. On the other hand, we obtain $\Delta M_{\chi_{c0}}\simeq 142.43$ MeV (Set I) and $\Delta M_{\chi_{c0}}\simeq 250.86$ MeV (Set IIb). Parameter Set I reproduces χ_{c0}, χ_{c1} and χ_{c2} as quasibound states while parameter Set IIb yields them as definite bound states.

It is of also interest to discuss the effects of the instanton vacuum on the hyperfine mass splitting. The contribution to the hyperfine mass splitting of each low-lying charmonium state is listed in Table 2.

While the instanton effects come into play significantly in $\Delta M_{\rm c\bar{c}}$, they turn out to be rather small in describing the hyperfine mass splittings of the charmonia. This might be due to the spin-dependent part of the potential from the instanton vacuum being almost an order of magnitude smaller than the central part. The tensor interaction contributes almost nothing to the results. As a result, the instanton effects on the hyperfine mass splittings are almost negligible. In order to obtain realistic results of the hyperfine mass splittings as well as of the charmonium masses, we need to include the Coulomb-like potential coming from the perturbative one gluon-exchange and the confining potential together with that from the instanton vacuum.

Table 1. Low-lying charmonium states from the instanton potential. Charm quark mass is set to be $m_{\rm c}=1275$ MeV.

	this work Set I $\bar{\rho}=1/3$ fm,$R=1$ fm [60, 71]/MeV	this work Set IIb $\bar{\rho}=0.36$ fm,$R=0.89$ fm [83–86]/MeV	experiment [73]/MeV
$M_{\eta_{\rm c}}$	2668.81	2753.64	2983.6±0.6
$M_{\rm J/\psi}$	2669.57	2755.36	3096.916±0.11
$M_{\chi_{c0}}$	2692.43	2800.86	3414.75±0.31
$M_{\chi_{c1}}$	2692.50	2801.11	3510.66±0.07
$M_{\chi_{c2}}$	2692.67	2801.70	3556.20±0.09

Table 2. Contributions to the hyperfine mass splittings of the low-lying charmonium states. Charm quark mass is set to be m_c=1275 MeV.

	this work Set I $\bar{\rho}$=1/3 fm, R=1 fm [60, 71]/MeV	this work Set IIb $\bar{\rho}$=0.36 fm,R=0.89 fm [83–86]/MeV	experiment [73]/MeV
$\Delta M_{J/\psi-\eta_c}$	0.72	1.72	113.32 ± 0.70
$\Delta M_{\chi_{c1}-\chi_{c0}}$	0.07	0.25	95.91 ± 0.32
$\Delta M_{\chi_{c2}-\chi_{c0}}$	0.24	0.84	141.45 ± 0.32
$\Delta M_{\chi_{c2}-\chi_{c1}}$	0.16	0.59	45.54 ± 0.11

Table 3. Low-lying bottomonium states from the instanton potential. Charm quark mass is set to be m_b=4180 MeV.

	this work Set I $\bar{\rho}$=1/3 fm, R=1 fm [60, 71]/MeV	experiment [73] /MeV
M_{η_b}	8454.58	9399.0±2.3
M_Υ	8454.76	9460.30±0.26
$M_{\chi_{b0}}$	8477.95	9859.44±0.52
$M_{\chi_{b1}}$	8477.97	9892.78±0.40
$M_{\chi_{b2}}$	8478.01	9912.21±0.40

4 Summary and outlook

In the present work, we aimed at investigating the instanton effects on the heavy-quark potential, based on the instanton liquid model. We first considered the heavy-quark propagator starting from the QCD Lagrangian, which is essential in deriving the heavy-quark potential. We showed briefly how to construct the heavy-quark potential from the instanton vacuum. Expanding the heavy-quark propagator in powers of the inverse mass of the heavy quark, we obtained the spin-dependent parts of the heavy-quark potential. We studied the dependence of the heavy-quark potential on the two essential parameters for the instanton vacuum, that is, the average size of the instanton ($\bar{\rho}$) and the distance between the instantons ($\bar{R}$). The results of the potential are very sensitive to the parameter $\bar{R}$, while they vary marginally with changes in $\bar{\rho}$. The spin-spin interaction shows r dependence similar to a Gaussian-type potential, which is distinguished from the point-like spin-spin interaction derived from perturbative QCD. The spin-orbit potential behaves like the spin-spin interaction, whereas the tensor potential is different. It increases until r reaches approximately 0.4 fm and then starts to fall off.

Having explicitly solved the Schrödinger equation with the heavy-quark potential purely induced by the instantons, we discussed the masses of the low-lying quarkonia. The instanton contribution to the hyperfine mass splitting turns out to be tiny due to the smallness of the spin-dependent part of the potential. We also discussed the dependence of the results on the intrinsic parameters of the instanton vacuum, i.e. the average size of the instanton and the distance between instantons.

It is of great importance to study carefully the mass spectra of the quarkonia and their decays by explicitly solving the Schrödinger equation, combining the heavy-quark potential derived in the present work with the confining and Coulomb potentials. Considering the fact that the instanton vacuum plays a key role in realizing chiral symmetry and its spontaneous breaking in QCD, nonperturbative gluon dynamics is expected to shed light on strong decays of quarkonia involving pions. Since the central part of the heavy-quark potential was derived by using the small packing parameter N/VN_c, we can obtain the corrections from the next-to-leading order $(N/VN_c)^2$. In principle, it is not that difficult to compute them. Starting from the instanton operator corresponding to the Wilson line (see Eq.(17) in Ref. [59]), we can consider the next-to-leading order in the expansion with respect to the small packing parameter of the instanton medium. Though the corrections from the next-to-leading order might be very small, one could use it for fine-tuning of the mass spectrum of the quarkonia. The corresponding investigations are under way.

HChK wants to express his gratitude to A. Hosaka, M. Oka, and Q. Zhao for very useful comments and discussions at "The 31st Reimei Workshop on Hadron Physics in Extreme Conditions at J-PARC". HChK owes also a debt of thanks to the late D. Diakonov and V. Petrov for invaluable discussions and suggestions.

Appendix A

Useful formulae

Using the instanton and anti-instanton fields

$$A_{I\mu}=\frac{x_\nu\bar{\eta}^a_{\mu\nu}\tau^a\rho^2}{x^2(x^2+\rho^2)},\qquad A_{\bar{I}\mu}=\frac{x_\nu\eta^a_{\mu\nu}\tau^a\rho^2}{x^2(x^2+\rho^2)},\tag{A1}$$

where $\bar{\eta}^a_{\mu\nu}$ and $\eta^a_{\mu\nu}$ denote the 't Hooft symbols [88], we can easily derive the path-ordered exponential as follows [59]

$$\begin{aligned}P\exp\left(\mathrm{i}\int_{-\infty}^{\infty}\mathrm{d}x_4A_{I4}\right)=&-\cos\left(\frac{\pi|\boldsymbol{z}|}{\sqrt{\rho^2+z^2}}\right)\\&-\mathrm{i}\frac{\boldsymbol{\tau}\cdot\boldsymbol{z}}{|\boldsymbol{z}|}\sin\left(\frac{\pi|\boldsymbol{z}|}{\sqrt{\rho^2+z^2}}\right),\end{aligned}\tag{A2}$$

which is used for deriving the heavy-quark potential and the instanton corrections to the heavy-quark mass.

The leading-order propagator given in Eq. (11) is the same as the path-ordered exponential, apart from the Dirac delta function. Thus, it is of great use to consider the identities derived in Ref. [58] for the path-order exponentials when we compute the spin-dependent parts of the heavy-quark potential. Defining the path-ordered exponential as

$$P(x_4,y_4):=P\exp\left(\mathrm{i}\int_{x_4}^{y_4}\mathrm{d}z_4A_4(z)\right),\tag{A3}$$

we have the following identities

$$\begin{aligned}&P(x_4,y_4)P(y_4,z_4)=P(x_4,z_4),\\&D_i(x_4)P(x_4,y_4)-P(x_4,y_4)D^i(y_4)\\=&\int_{y_4}^{x_4}\mathrm{d}zP(x_4,z)E_i(z)P(z,y_4),\\&P(\boldsymbol{y},t;\boldsymbol{x},t)D_i(\boldsymbol{x},t)P(\boldsymbol{x},t;\boldsymbol{y},t)=D_i(\boldsymbol{y},t)\\-&\epsilon_{ijk}\int_0^1\mathrm{d}\alpha(x-y)_j[P(\boldsymbol{y},t;\boldsymbol{z},t)B_k(\boldsymbol{z},t)P(\boldsymbol{z},t;\boldsymbol{y},t)],\end{aligned}\tag{A4}$$

where $\boldsymbol{z}=\alpha\boldsymbol{y}+(1-\alpha)\boldsymbol{x}$. D_i denotes the spatial component of the covariant derivative. When time t goes to infinity, i.e. $t=\pm\frac{T}{2}\to\infty$, the third identity is simplified to be

$$\lim_{|t|\to\infty}P(\boldsymbol{y},t;\boldsymbol{x},t)\boldsymbol{D}(\boldsymbol{x},t)P(\boldsymbol{x},t;\boldsymbol{y},t)=\mathrm{i}\nabla_y.\tag{A5}$$

References

1 S. K. Choi et al (Belle Collaboration), Phys. Rev. Lett., **91**: 262001 (2003)
2 B. Aubert et al (BaBar Collaboration), Phys. Rev. D, **71**: 071103 (2005)
3 B. Aubert et al (BaBar Collaboration), Phys. Rev. Lett., **95**: 142001 (2005)
4 K. Abe et al (Belle Collaboration), Phys. Rev. Lett., **98**: 082001 (2007)
5 S. K. Choi et al (Belle Collaboration), Phys. Rev. Lett., **100**: 142001 (2008)
6 A. Bondar et al (Belle Collaboration), Phys. Rev. Lett., **108**: 122001 (2012)
7 Z. Q. Liu et al (Belle Collaboration), Phys. Rev. Lett., **110**: 252002 (2013)
8 M. Ablikim et al (BESIII Collaboration), Phys. Rev. Lett., **110**: 252001 (2013)
9 M. Ablikim et al (BESIII Collaboration), Phys. Rev. Lett., **111**: 242001 (2013)
10 R. Aaij et al (LHCb Collaboration), Phys. Rev. Lett., **110**: 222001 (2013)
11 M. Ablikim et al (BESIII Collaboration), Phys. Rev. Lett., **112**: 022001 (2014)
12 R. Aaij et al (LHCb Collaboration), Phys. Rev. Lett., **112**: 222002 (2014)
13 R. Aaij et al (LHCb Collaboration), Phys. Rev. D, **92**: 112009 (2015)
14 B. Aubert et al (BaBar Collaboration), Phys. Rev. Lett., **101**: 071801 (2008) (Phys. Rev. Lett., **102**: 029901 (2009))
15 B. Aubert et al (BaBar Collaboration), Phys. Rev. Lett., **103**: 161801 (2009)
16 G. Bonvicini et al (CLEO Collaboration), Phys. Rev. D, **81**: 031104 (2010)
17 R. Mizuk et al (Belle Collaboration), Phys. Rev. Lett., **109**: 232002 (2012)
18 S. Dobbs, Z. Metreveli, K. K. Seth, A. Tomaradze and T. Xiao, Phys. Rev. Lett., **109**: 082001 (2012)
19 U. Tamponi et al (Belle Collaboration), Phys. Rev. Lett., **115**: 142001 (2015)
20 R. Mizuk et al (Belle Collaboration), Phys. Rev. Lett., **117**: 142001 (2016)
21 R. Aaij et al (LHCb Collaboration), Phys. Rev. Lett., **115**: 072001 (2015)
22 A. J. Bevan et al (BaBar and Belle Collaborations), Eur. Phys. J. C, **74**: 3026 (2014)
23 A. Andronic et al, Eur. Phys. J. C, **76**: 107 (2016)
24 C. Z. Yuan (BESIII Collaboration), Front. Phys. China, **10**: 101401 (2015)
25 C. Z. Yuan (Belle Collaboration), arXiv:1512.03281 (hep-ex)
26 E. S. Swanson, Phys. Rept., **429**: 243 (2006)
27 E. Eichten, S. Godfrey, H. Mahlke and J. L. Rosner, Rev. Mod. Phys., **80**: 1161–1193 (2008)
28 M. B. Voloshin, Prog. Part. Nucl. Phys., **61**: 455–511 (2008)
29 N. Brambilla et al, Eur. Phys. J. C, **71**: 1534 (2011)
30 S. L. Olsen, Front. Phys., **10**: 101401 (2015)
31 A. A. Penin, arXiv:0905.4296 (hep-ph)
32 S. Recksiegel and Y. Sumino, Phys. Lett. B, **578**: 369–375 (2004)
33 B. A. Kniehl, A. A. Penin, A. Pineda, V. A. Smirnov and M. Steinhauser, Phys. Rev. Lett., **92**: 242001 (2004) (Phys. Rev. Lett., **104**: 242001 (2010))
34 C. Patrignani, T. K. Pedlar and J. L. Rosner, Ann. Rev. Nucl. Part. Sci., **63**: 21–44 (2013)
35 E. Eichten, K. Gottfried, T. Kinoshita, J. B. Kogut, K. D. Lane and T. M. Yan, Phys. Rev. Lett., **34**: 369–372 (1975)
36 E. Eichten, K. Gottfried, T. Kinoshita, K. D. Lane and T. M. Yan, Phys. Rev. D, **17**: 3090–3117 (1978) (Phys. Rev. D, **21**: (1980) 313)
37 L. Susskind, "Coarse Grained Quantum Chromodynamics," in Weak and Electromagnetic Interactions at high energies: Proceedings. Edited by Roger Balian and Christopher H. Llewellyn Smith (N.Y., North-Holland, 1977)
38 T. Appelquist, M. Dine and I. J. Muzinich, Phys. Lett. B, **69**: 231–236 (1977)
39 T. Appelquist, M. Dine and I. J. Muzinich, Phys. Rev. D, **17**: 2074–2081 (1978)
40 W. Fischler, Nucl. Phys. B, **129**: 157–174 (1977)
41 M. Peter, Phys. Rev. Lett., **78**: 602–605 (1997)

42 M. Peter, Nucl. Phys. B, **501**: 471–494 (1997)
43 Y. Schröder, Phys. Lett. B, **447**: 321–326 (1999)
44 A. V. Smirnov, V. A. Smirnov and M. Steinhauser, Phys. Rev. Lett., **104**: 112002 (2010)
45 C. Anzai, Y. Kiyo and Y. Sumino, Phys. Rev. Lett., **104**: 112003 (2010)
46 K. G. Wilson, Phys. Rev. D, **10**: 2445–2459 (1974)
47 G. S. Bali and K. Schilling, Phys. Rev. D, **46**: 2636–2646 (1992)
48 S. P. Booth et al (UKQCD Collaboration), Phys. Lett. B, **294**: 385–390 (1992)
49 G. S. Bali, K. Schilling and A. Wachter, Phys. Rev. D, **55**: 5309–5324 (1997)
50 U. Glassner et al (SESAM Collaboration), Phys. Lett. B, **383**: 98–104 (1996)
51 G. S. Bali, K. Schilling and A. Wachter, Phys. Rev. D, **56**: 2566–2589 (1997)
52 G. S. Bali, Phys. Rept., **343**: 1–136 (2001)
53 T. Kawanai and S. Sasaki, Phys. Rev. D, **89**: 054507 (2014)
54 T. Kawanai and S. Sasaki, Phys. Rev. D, **92**: 094503 (2015)
55 A. A. Belavin, A. M. Polyakov, A. S. Schwartz and Y. S. Tyupkin, Phys. Lett. B, **59**: 85–87 (1975)
56 F. Wilczek and A. Zee, Phys. Rev. Lett., **40**: 83–86 (1978)
57 C. G. Callan, Jr., R. F. Dashen, D. J. Gross, F. Wilczek and A. Zee, Phys. Rev. D, **18**: 4684–4692 (1978)
58 E. Eichten and F. Feinberg, Phys. Rev. D, **23**: 2724–2744 (1981)
59 D. Diakonov, V. Y. Petrov and P. V. Pobylitsa, Phys. Lett. B, **226**: 372–376 (1989)
60 D. Diakonov and V. Y. Petrov, Nucl. Phys. B, **245**: 259–292 (1984)
61 D. Diakonov and V. Y. Petrov, Nucl. Phys. B, **272**: 457–489 (1986)
62 D. Diakonov, Prog. Part. Nucl. Phys., **51**: 173–222 (2003)
63 M. Fukushima, H. Suganuma, A. Tanaka, H. Toki and S. Sasaki, Nucl. Phys. Proc. Suppl., **63**: 513–515 (1998)
64 D. Chen, R. C. Brower, J. W. Negele and E. V. Shuryak, Nucl. Phys. Proc. Suppl., **73**: 512–514 (1999)
65 D. Diakonov and V. Petrov, Phys. Scripta, **61**: 536–543 (2000)
66 H. Georgi, Phys. Lett. B, **240**: 447–450 (1990)
67 T. Mannel, W. Roberts and Z. Ryzak, Nucl. Phys. B, **368**: 204–217 (1992)
68 L. L. Foldy and S. A. Wouthuysen, Phys. Rev., **78**: 29–36 (1950)
69 J. G. Körner and G. Thompson, Phys. Lett. B, **264**: 185–192 (1991)
70 P. V. Pobylitsa, Phys. Lett. B, **226**: 387–392 (1989)
71 E. V. Shuryak, Nucl. Phys. B, **203**: 93–115 (1982)
72 H. D. Son, S. i. Nam and H.-Ch. Kim, Phys. Lett. B, **747**: 460–467 (2015)
73 C. Patrignani et al (Particle Data Group), Chin. Phys. C, **40**: 100001 (2016)
74 A. Gray, I. Allison, C. T. H. Davies, E. Dalgic, G. P. Lepage, J. Shigemitsu and M. Wingate, Phys. Rev. D, **72**: 094507 (2005)
75 T. W. Chiu et al (TWQCD Collaboration), Phys. Lett. B, **651**: 171–176 (2007)
76 S. Meinel, Phys. Rev. D, **82**: 114502 (2010)
77 R. J. Dowdall et al (HPQCD Collaboration), Phys. Rev. D, **85**: 054509 (2012)
78 J. L. Richardson, Phys. Lett. B, **82**: 272–274 (1979)
79 W. Buchmuller and S. H. H. Tye, Phys. Rev. D, **24**: 132–156 (1981)
80 H.-Ch. Kim, M. M. Musakhanov and M. Siddikov, Phys. Lett. B, **633**: 701–709 (2006)
81 K. Goeke, M. M. Musakhanov and M. Siddikov, Phys. Rev. D, **76**: 076007 (2007)
82 K. Goeke, H.-Ch. Kim, M. M. Musakhanov and M. Siddikov, Phys. Rev. D, **76**: 116007 (2007)
83 M. C. Chu, J. M. Grandy, S. Huang and J. W. Negele, Phys. Rev. D, **49**: 6039–6051 (1994)
84 J. W. Negele, Nucl. Phys. Proc. Suppl., **73**: 92–104 (1999)
85 T. A. DeGrand, Phys. Rev. D, **64**: 094508 (2001)
86 P. Faccioli and T. A. DeGrand, Phys. Rev. Lett., **91**: 182001 (2003)
87 N. Brambilla, A. Pineda, J. Soto and A. Vairo, Rev. Mod. Phys., **77**: 1423–1496 (2005)
88 G. 't Hooft, Phys. Rev. D, **14**: 3432–3450 (1976) (Phys. Rev. D, **18**: 2199(1978))
89 E. Hiyama, Y. Kino and M. Kamimura, Prog. Part. Nucl. Phys., **51**: 223 (2003)